PAPER • OPEN ACCESS

The comparison of two continuum damage mechanics-based material models for formability prediction of AA6082 under hot stamping conditions

To cite this article: Z Shao *et al* 2017 *J. Phys.: Conf. Ser.* **896** 012056

View the article online for updates and enhancements.

The comparison of two continuum damage mechanics-based material models for formability prediction of AA6082 under hot stamping conditions

Z Shao[1]**, N Li**[1] **and J Lin**[1]

[1]Department of Mechanical Engineering, Imperial College London, London, SW7 2AZ, UK

E-mail: n.li09@imperial.ac.uk

Abstract. The hot stamping and cold die quenching process has experienced tremendous development in order to obtain shapes of structural components with great complexity in automotive applications. Prediction of the formability of a metal sheet is significant for practical applications of forming components in the automotive industry. Since microstructural evolution in an alloy at elevated temperature has a large effect on formability, continuum damage mechanics (CDM)-based material models can be used to characterise the behaviour of metals when a forming process is conducted at elevated temperatures. In this paper, two sets of unified multi-axial constitutive equations based on material's stress states and strain states, respectively, were calibrated and used to effectively predict the thermo-mechanical response and forming limits of alloys under complex hot stamping conditions. In order to determine and calibrate the two material models, formability tests of AA6082 using a developed novel biaxial testing system were conducted at various temperatures and strain rates under hot stamping conditions. The determined unified constitutive equations from experimental data are presented in this paper. It is found that both of the stress-state based and strain-state based material models can predict the formability of AA6082 under hot stamping conditions.

1. Introduction

The automotive industry is facing a huge global challenge to reduce fuel consumption and minimise environmental pollution from vehicle emissions. The hot stamping and cold die quenching process has been developed to obtain components with great complexity and high mechanical properties. The control of heating rate, cooling rate, forming speed and metallic sheet temperature is critical for the success of these processes.

Formability tests with special tooling and test procedures are usually needed to evaluate the formability of a metal sheet. The forming limit diagram (FLD) is a conventional tool to illustrate the formability of sheet metals. It is very difficult to obtain FLDs of metals under hot stamping and cold die quenching conditions by using conventional methods, since the cooling which occurs prior to deformation and constant deformation temperature, strain rate and strain path are not easy to obtain. A novel formability testing system have been proposed and developed to determine formability of metals experimentally for hot sheet stamping applications [1].

Experimentally determination [2] of the FLD of a material is time-consuming and costly, which restricts the number of tests to be conducted. Although various analytical and numerical models have been developed for formability prediction, most of them are applicable to only ambient conditions. Banabic et al. [3] reviewed primary models in the field of forming limit prediction at room

temperature from four aspects, namely new constitutive equations used for limit strain computation, polycrystalline models, ductile damage models and advanced numerical models for non-linear strain path or various process parameters. For applications at elevated temperatures, Hora [4] applied the modified maximum force criterion (MMFC) to predict FLD of stainless steel at elevated temperatures from 500 ℃ to 850 ℃ by introducing temperature dependent hardening curves. This model is robust and reliable only when the yield locus of the material is elliptical [5]. Abedrabbo et al. [6] introduced a modified power law flow rule which included temperature effects and assumed isotropic hardening behaviour in the material. Combining YLD96, YLD200-2d anisotropic yield functions with the M-K model [7], FLDs of aluminium alloys can be predicted. Storen and Rice [8] used a bifurcation analysis to describe the behaviour of the FLC by imposing force equilibrium between the necked and non-necked region of the metal. Based on Storen and Rice's Vertex theory and Logon-Hosford yield criterion, Min et al. [9] proposed a model for the prediction of FLD of steel 22MnB5 at elevated temperatures. The constitutive behaviour is usually described with macroscopic phenomenological material models; however, microstructural evolution is significant at elevated temperatures, which greatly affects mechanical properties. Therefore, advanced material models are needed for the prediction of forming limits of metals under hot stamping conditions.

The aim of this research is to calibrate continuum damage mechanics (CDM)-based material models to be used for formability prediction of alloys, based on stress states and strain states, respectively, under hot stamping conditions, and to compare the accuracy of formability prediction by the two material models.

2. Development of CDM-based material models

The CDM-based material model describing viscoplastic behaviour contains formulations of the unified constitutive equations developed based on the mechanisms of dislocation-driven evolution processes, including work hardening, static and dynamic recovery and plasticity-induced ductile damage. It models time-dependent phenomena, including strain rate effects, recovery and damage evolution [10]. An Arrhenius-type equation is used to formulate temperature dependent parameters.

$$\dot{\varepsilon}_p = \left(\frac{\left| \frac{\sigma_e}{1-\omega} \right| - R - k}{K} \right)^{n_1} \quad (1) \qquad \dot{\varepsilon}_{ij}^P = \frac{3}{2}\frac{S_{ij}}{\sigma_e}\dot{\varepsilon}_P \quad (2) \qquad \dot{R} = 0.5 B \overline{\rho}^{-0.5}\dot{\overline{\rho}} \quad (3)$$

$$\dot{\overline{\rho}} = A\left(1-\overline{\rho}\right)\left|\dot{\varepsilon}_P\right| - C\overline{\rho}^{n_2} \quad (4) \qquad \sigma_{ij} = \left(1-\omega\right) D_{ijkl}\left(\varepsilon_{ij} - \varepsilon_{ij}^P\right) \quad (5)$$

Equation (1) is the flow rule, in which plastic strain rate $\dot{\varepsilon}_P$ is formulated by using the traditional power law with damage ω taken into account. k represents the initial yield point and R represents the isotropic hardening. In Equation (2), σ_e is effective stress, S_{ij} are the deviatoric stress components. Isotropic hardening R in Equation (3) is a function of the normalized dislocation density $\overline{\rho}$ ($\overline{\rho} = 1 - \rho_0 / \rho$, where ρ_0 is the initial dislocation density and ρ is the instantaneous dislocation density during deformation), where $\overline{\rho}$ is given by Equation (4) which represents the accumulation of dislocations due to plastic flow and dynamic and static recoveries. The flow stress is defined to include the effect of damage in Equation (5). D_{ijkl} is the elastic matrix of a material. K, k, n_1, B, C, and E temperature dependent parameters defined by:

$$K = K_0 \exp\left(\frac{Q_K}{R_g T}\right) \quad (6) \qquad k = k_0 \exp\left(\frac{Q_k}{R_g T}\right) \quad (7) \qquad n_1 = n_{1_0} \exp\left(\frac{Q_{n_1}}{R_g T}\right) \quad (8)$$

$$B = B_0 \exp\left(\frac{Q_B}{R_g T}\right) \quad (9) \qquad C = C_0 \exp\left(-\frac{Q_C}{R_g T}\right) \quad (10) \qquad E = E_0 \exp\left(\frac{Q_E}{R_g T}\right) \quad (11)$$

Where R_g is the universal gas constant, T is the absolute temperature, K_0, k_0, n_{1_0}, B_0, C_0, E_0, Q_K, Q_k, Q_{n_1}, Q_B, Q_C, and Q_E are material constants to be determined from experimental data.

2.1. Stress-state based damage equation

In metal forming processes, stress states of deformation vary depending on forming process and conditions. A stress state can be characterised as comprising principal stresses, hydrostatic stress which does not affect plastic deformation, and deviatoric stresses associated with plastic deformation. A particular characterisation can be used to assess the form of deformation arising under different loading conditions, such as simple tension, compression and plane strain.

In order to describe the effects of stress states on the damage evolution of a material, stress state dependent damage evolution equation was proposed for alloys for hot stamping applications, as shown in Equation (12). The damage evolution $\dot{\omega}$ in Equation (12) used for AA6082 was based on the growth and nucleation of voids around particles.

$$\dot{\omega} = \frac{\Delta}{(\alpha_1 + \alpha_2 + \alpha_3)^\varphi} \left(\frac{\alpha_1 \sigma_1 + 3\alpha_2 \sigma_H + \alpha_3 \sigma_e}{\sigma_e} \right)^\varphi \frac{\eta_1}{(1-\omega)^{\eta_3}} (\dot{\varepsilon}_P)^{\eta_2} \tag{12}$$

where σ_1 is the maximum principal stress, σ_H is hydrostatic stress, σ_e is effective stress, α_1, α_2, α_3 and φ are material constants. α_1, α_2 and α_3 are weighting parameters to control the effects of the maximum principal stress σ_1, hydrostatic stress σ_H and effective stress σ_e, respectively. Any values of α_1, α_2 and α_3 could be set to zero for modelling the behaviour of various metals and forming processes, which means that the corresponding stress term does not contribute to damage evolution for the material. Temperature dependent parameters are defined by:

$$\eta_1 = \eta_{1_0} \exp\left(-\frac{Q_{\eta_1}}{R_g T} \right) \quad (13) \qquad \eta_2 = \eta_{2_0} \exp\left(\frac{Q_{\eta_2}}{R_g T} \right) \quad (14) \qquad \eta_3 = \eta_{3_0} \exp\left(\frac{Q_{\eta_3}}{R_g T} \right) \quad (15)$$

where η_{1_0}, η_{2_0}, η_{3_0}, Q_{η_1}, Q_{η_2} and Q_{η_3} are material constants.

Δ is a factor to adjust the global position of a curve in an FLD. It is a strain rate dependent and also temperature dependent parameter:

$$\Delta = \Delta_{11} \exp\left(\frac{\Delta_{12}}{T} \right) + \Delta_{21} \exp\left(\Delta_{22} \dot{\varepsilon}_e \right) \tag{16}$$

where, Δ_{11}, Δ_{12}, Δ_{21} and Δ_{22} are material constants, T is the absolute temperature, $\dot{\varepsilon}_e$ is the effective strain rate. The damage rate exponent φ is introduced in this equation to mathematically control the profile shape of a forming limit curve. It is a temperature dependent parameter:

$$\varphi = \varphi_{11} \exp\left(-\frac{\varphi_{12}}{T} \right) \tag{17}$$

where φ_{11} and φ_{12} are material constants, T is the absolute temperature.

2.2. Strain-state based damage equation

A typical FLD is the plot of minor strain and major strain under different strain paths. In order to describe the effects of strain states on the damage evolution of a material, a principal strain dependent damage evolution equation was proposed for alloys under hot stamping conditions. For this material model, the flow rule, working hardening and dislocation density evolution law remain the same as Equations (1)-(11). A new equation is proposed to replace Equation (12) in order to describe the effects of principal strains on the damage evolution [11]:

$$\dot{\omega} = \left[\frac{\Delta^*}{\left(\mu_1 - 0.5\mu_2 \right)^\phi} \right] \left(\frac{\mu_1 \varepsilon_1 + \mu_2 \varepsilon_2}{\gamma + \varepsilon_P} \right)^\phi \frac{\eta_1}{\left(1 - \omega \right)^{\eta_3}} \left(\dot{\varepsilon}_P \right)^{\eta_2} \tag{18}$$

where μ_2 and γ are material constants, μ_1 and ϕ are defined as temperature dependent parameters, as shown in Equation (19)-(20), Δ^* is a temperature and also strain rate dependent parameter, presented in Equation (21).

$$\mu_1 = \mu_{11} \exp\left(-\frac{\mu_{12}}{T} \right) \tag{19}$$

$$\phi = \phi_{11} \exp\left(-\frac{\phi_{12}}{T} \right) \tag{20}$$

$$\Delta^* = \Delta_{11}^* \exp\left(\frac{\Delta_{12}^*}{T} \right) + \Delta_{21}^* \exp\left(\Delta_{22}^* \dot{\varepsilon}_e \right) \tag{21}$$

where μ_{11}, μ_{12}, ϕ_{11}, ϕ_{12}, Δ_{11}^*, Δ_{12}^*, Δ_{21}^* and Δ_{22}^* are material constants, T is the absolute temperature, $\dot{\varepsilon}_e$ is the effective strain rate. The parameters μ_1 and μ_2 are used to calibrate the effects of major strain and minor strain on the damage evolution. The values of μ_1 and μ_2 are suggested to be in the range of 0-1.0. ϕ is introduced in Equation (20) to control the intensity of the effects of principal strains on the damage evolution, thus to control the predicted FLD of the material.

3. Determination of the constitutive equations

3.1. Experimental Programme
A novel in-plane biaxial testing system had been developed to obtain FLDs of alloys for hot stamping applications in this study [1]. A biaxial testing apparatus had been invented and patented for using on the Gleeble thermo-mechanical testing machine to enable biaxial tensile testing. Testing parameters, such as heating rate, cooling rate, deformation temperature and strain rate, can be controlled precisely to simulate the hot stamping conditions and to reduce measurement errors of FLD results. Different proportional strain paths can be achieved by this apparatus and friction effects on FLD can be avoided. One type of cruciform specimen was proposed for the biaxial testing.

In this paper, commercial AA6082 was used for the formability tests. The material was heated to the solution heat treatment temperature of 535 ℃ with a heating rate of 30 ℃/s, soaked for 1 minute, and then cooled to a designated temperature in the range of 370-510 ℃ at a cooling rate of 100 ℃/s. The formability tests were conducted at constant effective strain rates at the range of 0.01-1/s under isothermal conditions. Strain path conditions include uniaxial, plane strain and biaxial tension.

### 3.2. Results of determined material constants
Material constants within the equations can be determined by fitting the computed FLDs to corresponding experimental data obtained from uniaxial tensile tests and formability tests at different deformation temperatures and strain rates after heating and cooling processes. The range of potential values for the constants was chosen based on their physical meanings and previous experience. The material constants for AA6082 in Equations (1)-(11) under hot stamping conditions calibrated by the trial and error method based on uniaxial tensile test results [12] are listed in Table 1. The material constants for AA6082 in Equations (12)-(21) can be calibrated based on formability test results under hot stamping conditions are listed in Table 2. Good agreement between experimental and computed FLDs can be seen for each forming limit curve in Figure 1 and Figure 2. Symbols in Figure 1 and Figure 2 represent the forming limits obtained experimentally under various strain paths from uniaxial, plane strain to biaxial straining states at different testing conditions [2].

Table 1 Material constants for Equations (1)-(11) for AA6082 under hot stamping conditions.

K_0 (MPa)	k_0 (MPa)	n_{0_1}	B_0 (MPa)	C_0	η_{1_0}	η_{2_0}	η_{3_0}
0.3624	0.5897	0.1018	4.8251	7.3057	2.4577	0.8357	0.2423
E_0 (MPa)	A	n_2	Q_K (J/mol)	Q_k (J/mol)	Q_{n_1} (J/mol)	Q_B (J/mol)	Q_C (J/mol)
249.69	0.19	1.83	25409.54	21692.97	17637.07	15698.86	2112.59
R (J/(molK))	Q_{η_1} (J/mol)	Q_{η_2} (J/mol)	Q_{η_3} (J/mol)	Q_E (J/mol)			
8.314	16273.24	837.80	22107.92	27987.42			
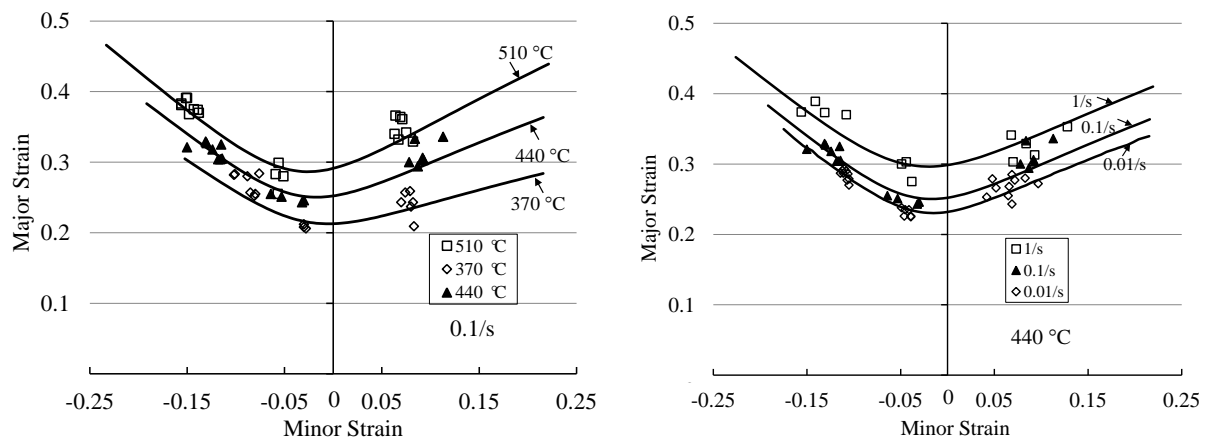
Figure 1 Comparison of experimental (symbols) and numerical integrated (solid curves) FLDs of AA6082 computed from the stress-state based material model.

Table 2 Material constants for Equations (12)-(21) for AA6082 under hot stamping conditions.

α_1	α_2	α_3	φ_{11}	φ_{12}	Δ_{11}	Δ_{12}	Δ_{22}	γ
0.450	-0.065	0.050	51.317	1579.47	0.343	5758.470	-5759.879	0.0035
μ_{11}	μ_{12}	μ_2	ϕ_{11}	ϕ_{12}	Δ_{11}^*	Δ_{12}^*	Δ_{21}^*	Δ_{22}^*
0.848	451.863	0.150	19.094	874.552	79.785	26.063	-81.107	3.517E-03
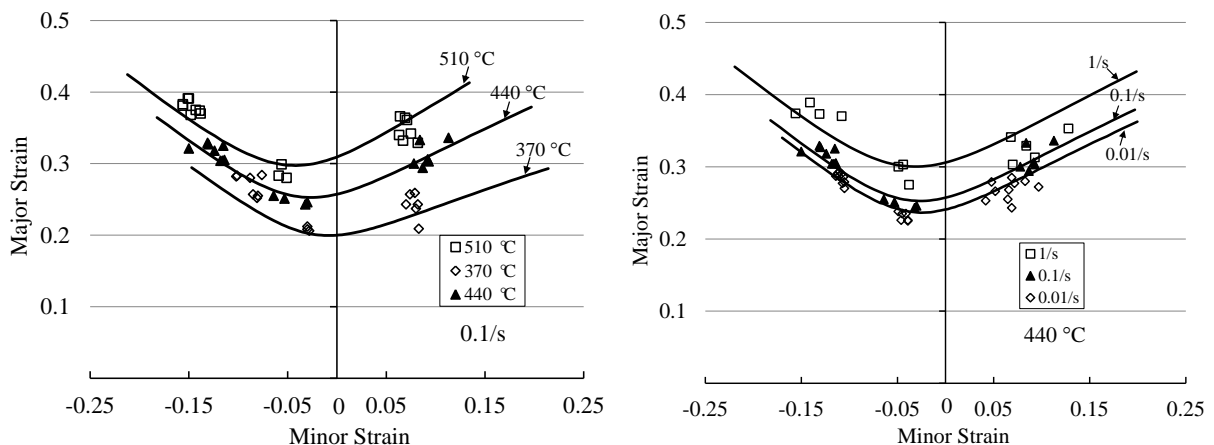
Figure 2 Comparison of experimental (symbols) and numerical integrated (solid curves) FLDs of AA6082 computed from the strain-state based material model.

4. Comparison of the two CDM-based material models

According to Figure 1 and Figure 2, the CDM material models based on stress states and strain states are both promising for modelling the formability of AA6082 under hot stamping conditions. It is noted that the stress-state dependent damage evolution equation is defined to apply to sheet metal forming process in which the plane stress situation exists, with a zero value of normal stress through the thickness direction. It represents damage mechanisms by introducing stress states into the damage evolution equation. This model is applicable for investigation on material response to applied force or stress. Compared with the stress-state dependent material model, the strain-state dependent material model can also be used to capture the features of a forming limit curve and it is more useful for practical application since formability is normally evaluated by an FLD which is strain-state based. This model is more applicable to study material response to applied displacement or strain. Both of the calibrated material models can provide accurate description of the thermo-mechanical deformation behaviour of alloys, thus for formability prediction of alloys under hot stamping conditions.

5. Conclusions

Two sets of unified viscoplastic-damage constitutive equations were adopted and calibrated from formability test results to model the thermo-mechanical properties of AA6082 under a range of forming temperatures of 370-510 ℃ and strain rates of 0.01-1/s for hot stamping applications. Both of the stress-state based and strain-state based damage equations are able to predict the formability of AA6082 under hot stamping conditions. The stress-state based damage evolution model has physical meaning to represent damage mechanisms and the principal strain-state based damage evolution model is more practical for engineering applications in terms of formability evaluation.

6. References

[1]   Shao Z, Li N, Lin J and Dean T A 2016 Development of a New Biaxial Testing System for Generating Forming Limit Diagrams for Sheet Metals Under Hot Stamping Conditions *Exp. Mech.* **56** 1489-500

[2]   Shao Z and Li N 2017 A novel biaxial testing apparatus for the determination of forming limit under hot stamping conditions *J. Visual. Exp.* **122**

[3]   Banabic D, Barlat F, Cazacu O and Kuwabara T 2010 Advances in anisotropy and formability *Int. J. Mat. Form.* **3** 165-89

[4]   Hora P and Tong L 2006 Prediction of forming limits in virtual sheet metal forming–yesterday, today and tomorrow. In: *Proc. of the FLC,* (Zurich) pp 8-23

[5]   Aretz H 2004 Numerical restrictions of the modified maximum force criterion for prediction of forming limits in sheet metal forming *Model. Simul. Mater. Sc.* **12** 677-92

[6]   Abedrabbo N, Pourboghrat F and Carsley J 2006 Forming of aluminum alloys at elevated temperatures – Part 2: Numerical modeling and experimental verification *Int. J. Plasticity* **22** 342-73

[7]   Marciniak Z and Kuczynski K 1967 Limit strains in the processes of stretch-forming sheet metal *Int. J. Mech. Sci.* **9** 609-20

[8]   Stören S and Rice J R 1975 Localized necking in thin sheets *Comp. Mater. Sci.* **23** 421–41

[9]   Min J, Lin J, Li J and Bao W 2010 Investigation on hot forming limits of high strength steel 22MnB5 *Comp. Mater. Sci.* **49** 326-32

[10]   Lin J, Mohamed M, Balint D and Dean T 2013 The development of continuum damage mechanics-based theories for predicting forming limit diagrams for hot stamping applications *Int. J. Damage Mech.* **23** 684-701

[11]   Mohamed M, Shi Z S, Lin J G, Dean T and Dear J 2015 Strain-Based Continuum Damage Mechanics Model for Predicting FLC of AA5754 under Warm Forming Conditions *Appl. Mech. Mater.* **784** 460-7

[12]   Shao Z, Li N and Lin J 2017 Strain measurement and error analysis in thermo-mechanical tensile tests of sheet metals for hot stamping applications *J. Mech. Eng. Sci.*